PREPRINT UCRL-80937

CONF-780822--2

Lawrence Livermore Laboratory

IMPROVED X-RAY FLUORESCENCE CAPABILITIES BY EXCITATION WITH HIGH INTENSITY POLARIZED X-RAYS

Richard W. Ryon and John D. Zahrt

July 1978

This paper was prepared for submission to Applications of X-ray Analysis *Conference*, University of Denver, Denver, Colorado, August 1-4, 1978.

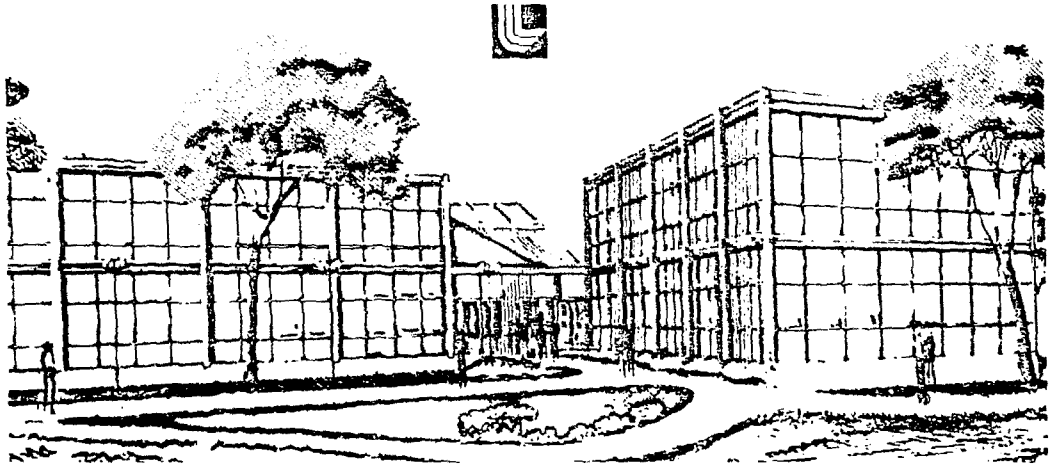

IMPROVED X-RAY FLUORESCENCE CAPABILITIES BY EXCITATION WITH HIGH INTENSITY POLARIZED X-RAYS*

Richard W. Ryon
Lawrence Livermore Laboratory
P.O. Box 808, L-325
Livermore, California 94550

John D. Zahrt
Northern Arizona University
Dept. of Chemistry
Box 5698
Flagstaff, Arizona 86011

Introduction and Review

Energy dispersive x-ray fluorescence is a useful tool for measuring major and trace elements in almost any kind of material. The method would have even greater application if a wider range of elements could be analyzed simultaneously with detection limits at least as good as obtained with a system tuned for a narrow range of elements. When analyzing bulk, low-Z matrix materials, one of the primary impediments is source radiation, which is scattered into the detector by the specimen being analyzed. The adverse effects of the scattered radiation are its contribution to the background signal ("noise") and its overwhelming contribution to the limited counting rate of the system electronics.

We have demonstrated that polarized x-radiation is a superior and practical excitation source. In our previous work, polarization was obtained by scattering a collimated beam of x-rays at an angle of 90° from boron carbide.[1] Fluorescent radiation is detected along a line perpendicular to the plane defined by the incident and scattered beams at the polarizer. Ideally, the only radiation detected is due to fluorescence in the specimen. Count rate limitations and background due to scattered source radiation are eliminated.

*Work performed under the auspices of the U.S. Department of Energy by the Lawrence Livermore Laboratory under contract number W-7405-ENG-48.

Polarization is obtained only with a commensurate loss in intensity. A high degree of polarization requires very tightly collimated beams, so that intensity approaches zero as the theoretical polarization approaches 100%. Therefore, the ideal case is not realized. It has been shown, however, that in such a system the detection limits are proportional to $\bar{\omega}^{-2}$, where $\bar{\omega}$ is the average angular divergence about the system angles (i.e., $\pi/2 \pm \bar{\omega}$). Therefore, the lowest detection limits are obtained by opening the collimator apertures until the system maximum counting rate is obtained.

When a standard 2500 watt Mo anode x-ray tube is used, the maximum counting rate is obtained when the polarization is about 85% (polarization $\approx 1-2\bar{\omega}^2$). For example, with collimator tubes approximately 1" in length, the corresponding diameters are about 3/8". Even though polarization is sacrificed, fluorescent radiation is enhanced over scattered radiation, as the latter is attenuated by the partial polarization factor ($\alpha \cos^2(\pi/2 \pm \bar{\omega}) \approx \bar{\omega}^2$). Using such a system, the detection limits for the elements K-Sr in NBS Standard Orchard Leaves range between about 3X to 1X lower as compared to the most favorable secondary exciter.

Polarizer Material Selection

The particular materials selected for the polarizer-scatterer depend upon the energy range of interest. The first consideration is the need for a high ratio of scatter relative to photoelectric absorption. This need infers a low Z material. However, the second consideration is that the interaction must take place over a limited region of space, namely the volume within the field of view of the collimators.

Equations of varying sophistication and accuracy have been derived to predict the scatter efficiences of materials.[2] One equation of intermediate complexity which proves to be quite useful is:

$$I_s = \frac{1}{4} I_o \left(\frac{\mu_s}{\mu_T}\right)\left(\frac{d\Omega}{4\pi}\right)^2 \left\{1 - \frac{1}{2d\mu_T\rho}\left(1 - e^{-2\sqrt{2}\mu_T\rho x_{max}}\right) - e^{-2\sqrt{2}\mu_T\rho x_{max}}\left(1 - \frac{\sqrt{2}\, x_{max}}{d}\right)\right\} \quad \text{(Eq. 1)}$$

where I_s = intensity of scattered radiation

μ_s = mass scatter coefficient (cm^2/g) = $\mu_T - \mu_{P.E.}$

μ_T = total mass absorption coefficient

$\mu_{P.E.}$ = mass photoelectric coefficient

$d\Omega$ = solid angle intercepted by the collimators

d = diameter of the collimators

x_{max} = scatterer thickness $\leq d/\sqrt{2}$

This equation is for monochromater radiation. The geometry modeled is square or rectangular collimators with angles of incidence and scatter = $\pi/4$ radians. Collimators used in our work are actually circular in cross section. The errors, however, are tolerable; for example, the calculated intensities are 2% and 10% too large at 4 and 40 keV respectively in boron carbide.

The degree of validity of Eq. 1 was experimentally evaluated at energies ranging from 3.7 to 76 keV. Fluorescent radiation from specimens following the scatterers was measured. Typical results are graphed in Figures 1 and 2 for CaKα and LuKα. The x-ray tube used was a W anode spectroscopy tube which may be operated up to 150 kV. The detector was high purity germanium. In Figures 1A and 2A, the intensities were calculated using equation 1; the interaction coefficients are those at the respective absorption edges. In Figures 1B and 2B, the intensities were calculated using Eq. 1 modified to include the tube spectrum (i.e., Kramer's rule) and the conversion of the incident radiation to fluorescence, all integrated from the absorption edge to the maximum operating voltage:

$$I_s = \frac{1}{4} T_o \left(\frac{d\Omega}{4\pi}\right)^2 \int_{V_k}^{V_o} \left(\frac{V_o}{V} - 1\right) V^2 \cdot \frac{\mu_s}{\mu_T} \cdot \left\{1 - \frac{1}{2d\mu_T\rho}\left(1 - e^{-2\sqrt{2}\mu_T\rho x_{max}}\right)\right.$$

$$\left. - e^{-2\sqrt{2}\mu_T\rho x_{max}}\left(1 - \frac{\sqrt{2}\, x_{max}}{d}\right)\right\} \frac{\mu_{P.E.}}{\mu_T}\, dV \qquad \text{(Eq. 2)}$$

Paradoxically, the simpler Eq. 1 fits the observed intensities somewhat better than Eq. 2.

The mathematical models can be used to guide the selection of scattering materials. Figures 3A and B illustrate the behavior of some typical materials as a function of energy using Eq. 1. It is seen the Be is an excellent material for low energy work, and that B_4C with its greater density is useful over a wide energy range. At the highest energies, medium-Z materials such as Fe are useful.

The goal stated at the outset is to obtain high sensitivity over a broad range of energies. This desire may be enhanced through the use of multi-layered scatter-polarizers. Successive layers of higher Z materials would efficiently scatter higher and higher energy x-rays, thereby providing broad-band polarized radiation to excite all elements simultaneously. The concept is illustrated in Figure 4.

Cylindrical Polarizer

We now have coming into operation a high intensity polarized x-ray source. The heart of this device is a cylindrical polarizer.[3] The concept is illustrated in Figure 5. The polarizer gathers radiation emitted from the anode over approximately 240°, which is equivalent to 2.7 $\pi\omega$ steradians. (With a collimated beam, the area is only $\pi\omega^2$ steradians.) Because of the larger area, the maximum counting rate will occur at a polarization of greater than 95%. We therefore anticipate further significant reductions in detection limits.

The new device is designed with versatility in mind. The cylindrical polarizer has a radius of 1.25", and a variable height initially set at 3/8". The degree of polarization may be varied on either side of 95% by changing the focal spot size of the electron beam, the height of the polarizer, and the diameter of the detector collimator. The primary radiation may also be selected by changing anodes.

We anticipate that we will be able to fully exploit the promise of energy dispersive analysis with this device - that is, to analyze a large number of elements simultaneously with high sensitivity.

Further advances may be anticipated for a narrow band of elements by using a crystalline polarizer selected to diffract the anode characteristic line at $2\theta = 90°$.[4] We would then have a high intensity, polarized, monochromatic source of x-rays, ideal for trace analysis. Work is continuing.

References

1. Richard W. Ryon, "Polarized Radiation Produced by Scatter for Energy Dispersive X-Ray Fluorescence Trace Analysis," Advances in X-Ray Analysis, Vol. 20, pp. 575-590 (1977), (H. F. McMurdie, et al, Eds., Plenum Press, New York and London).

2. John D. Zahrt and Richard W. Ryon, Scatter Efficiencies for Polarized X-Ray Sources, to be published.

3. Richard H. Howell, William L. Pickles, and James L. Cate, Jr., "X-Ray Fluorescence Experiments with Polarized X-Rays," Advances in X-Ray Analysis, Vol. 18, pp. 265-277 (1974), (W. H. Pickles, et al, Eds., Plenum Press, New York and London).

4. H. Aiginger, P. Wobrauschek, and C. Brauner, "Energy Dispersive Fluorescence Analysis using Bragg-Reflected Polarized X-Rays," Measurement, Detection, and Control of Environmental Pollutants, International Atomic Energy Agency, Vienna, 1976, pp. 197-212.

FIGURE 1A

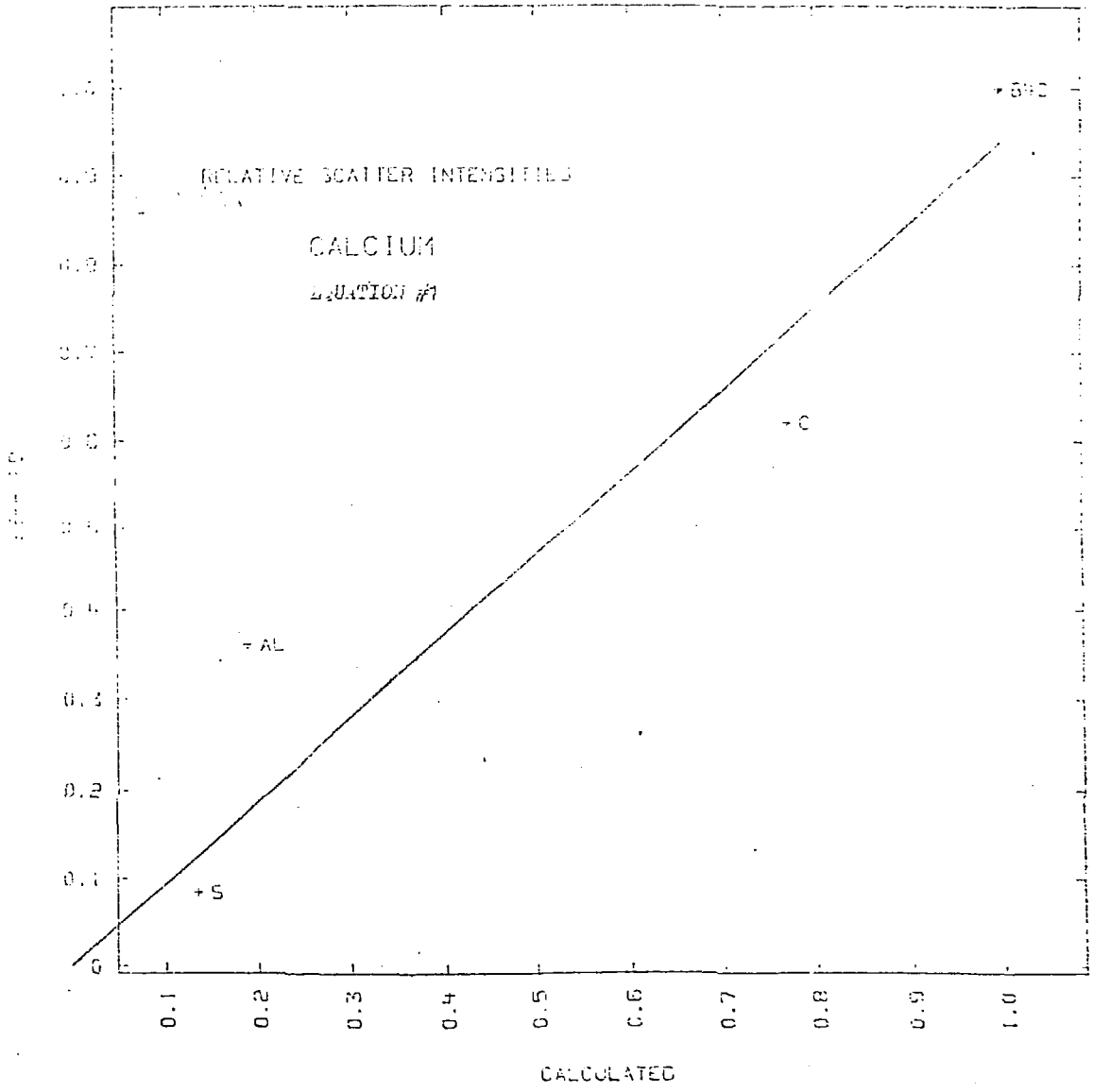

FIBURE 13

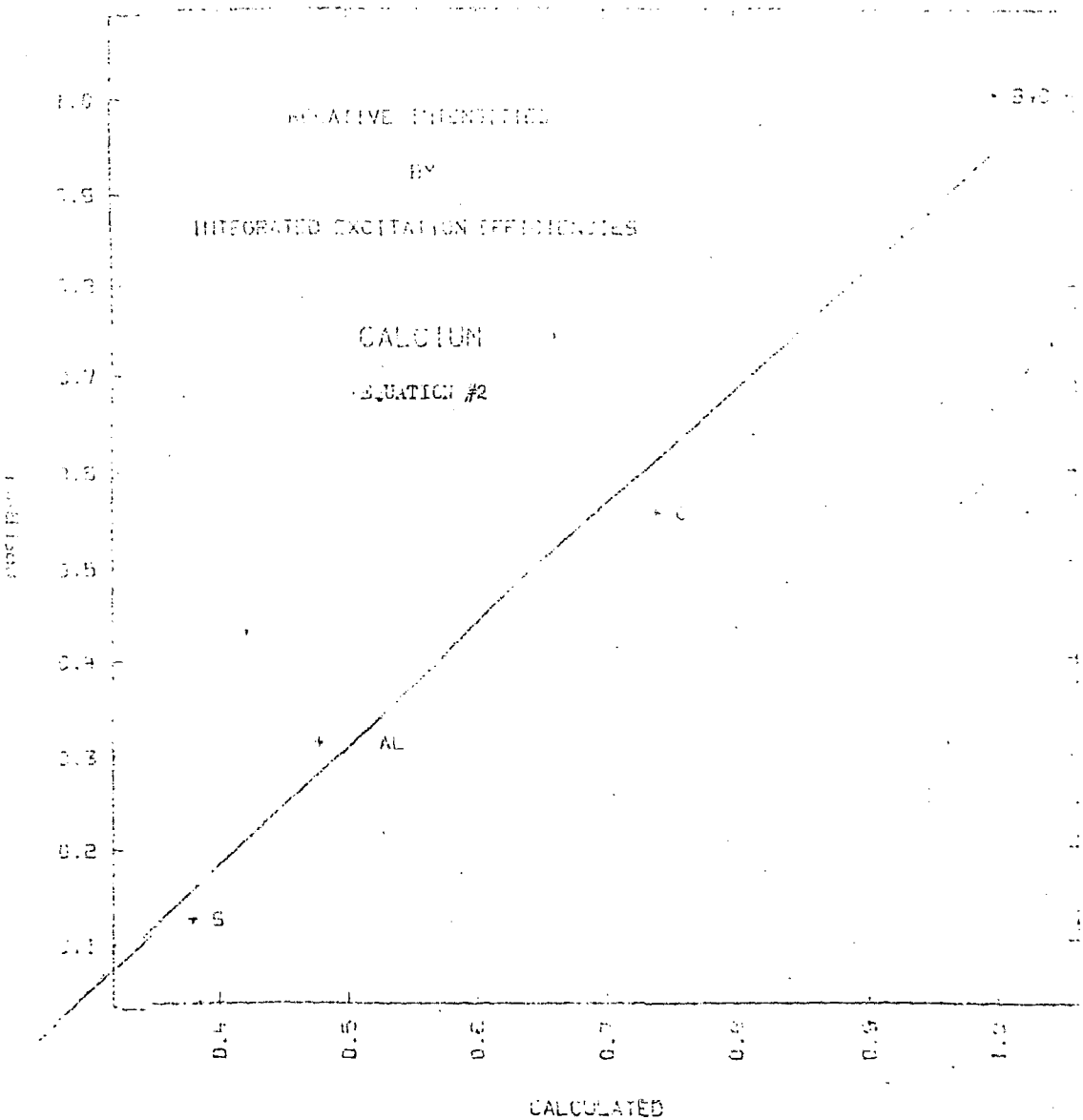
RELATIVE PRIORITIES
BY
INTEGRATED EXCITATION EFFICIENCIES
CALCIUM
EQUATION #2
1.0
0.9
0.8
0.7
0.6
0.5
0.4
0.3
0.2
0.1
S
AL
C
CALCULATED

FIGURE 2A

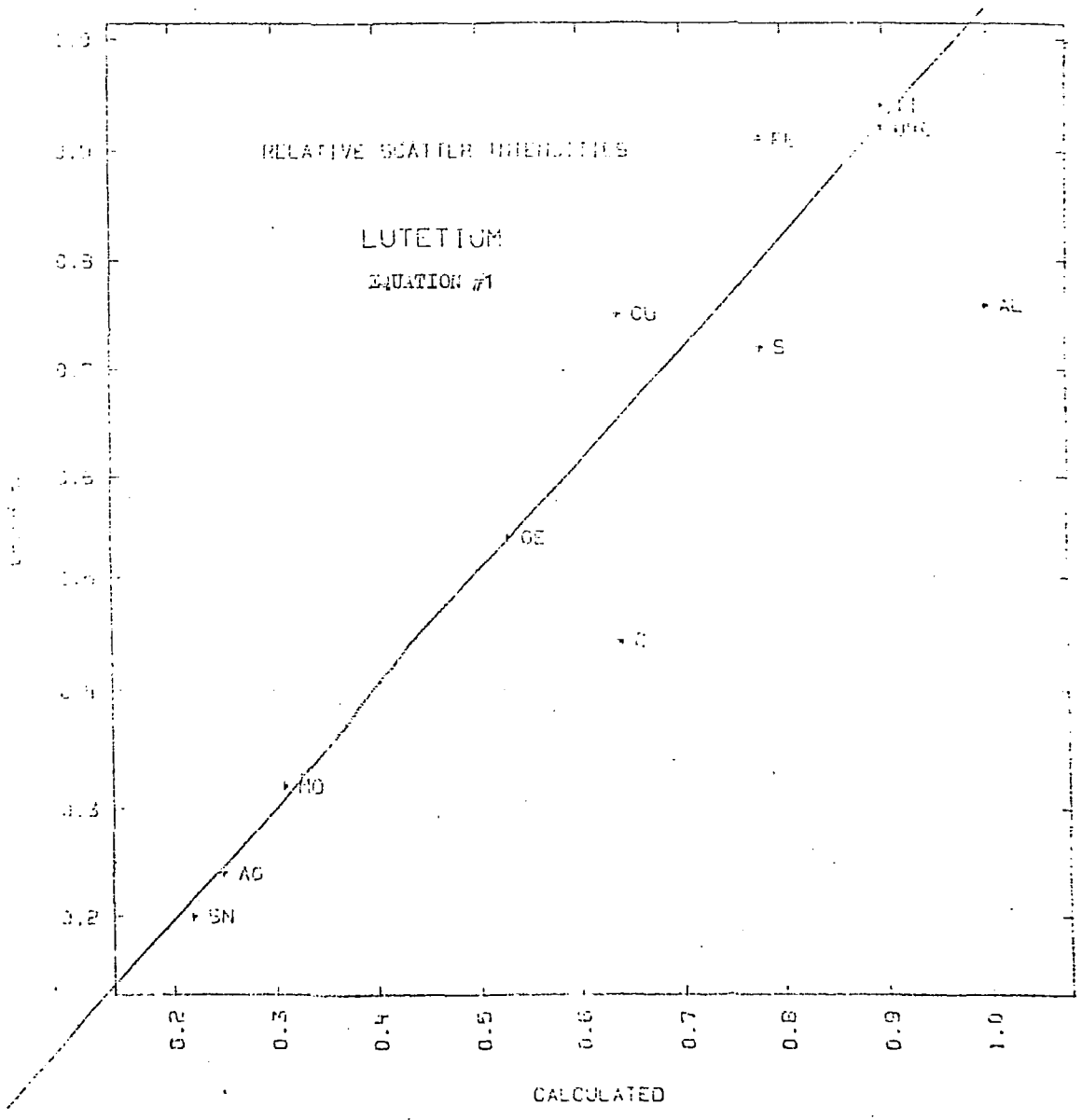
RELATIVE SCATTER INTENSITIES
LUTETIUM
EQUATION #1
CU
AL
S
GE
MO
AG
SN
0.2
0.3
0.4
0.5
0.6
0.7
0.8
0.9
1.0
CALCULATED

FIGURE 23

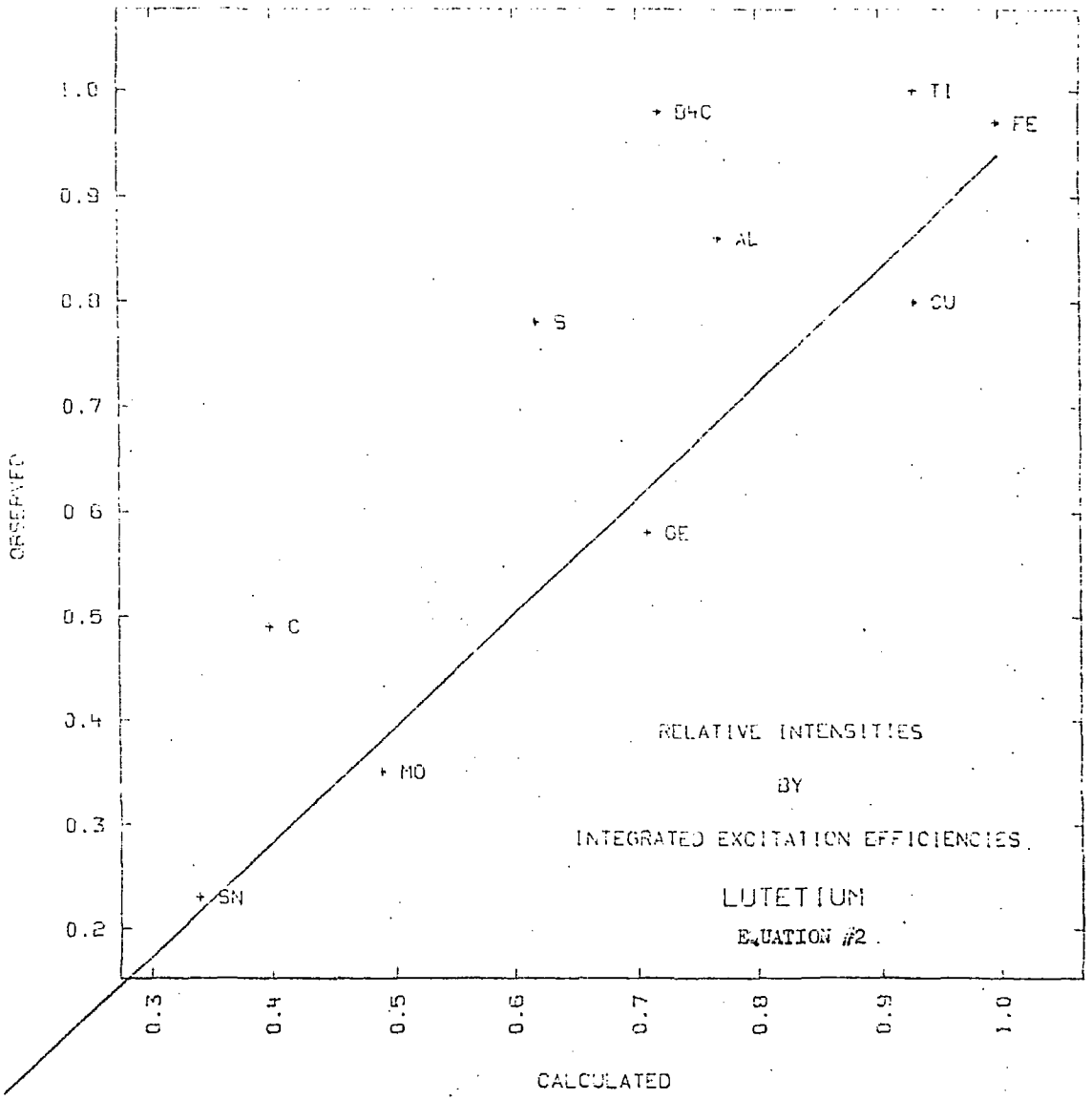
1.0
0.9
0.8
0.7
0.6
0.5
0.4
0.3
0.2
OBSERVED
0.3
0.4
0.5
0.6
0.7
0.8
0.9
1.0
CALCULATED
+ TI
+ DHC
+ FE
+ AL
+ CU
+ S
+ GE
+ C
+ MO
+ SN
RELATIVE INTENSITIES
BY
INTEGRATED EXCITATION EFFICIENCIES
LUTETIUM
EQUATION #2

FIGURE 3A

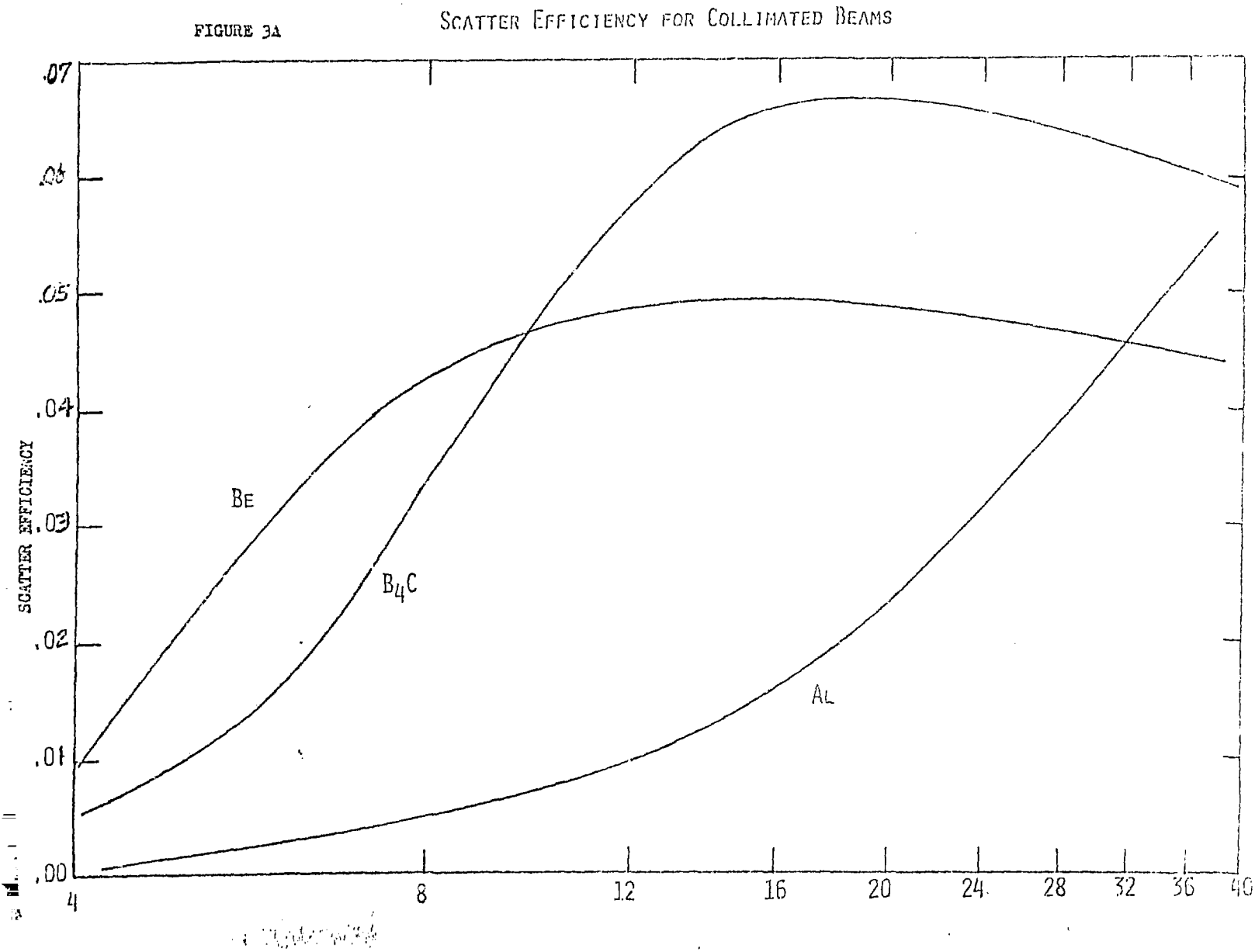
SCATTER EFFICIENCY FOR COLLIMATED BEAMS
SCATTER EFFICIENCY
.07
.06
.05
.04
.03
.02
.01
.00
4
8
12
16
20
24
28
32
36
40
BE
B4C
AL

FIGURE 3B

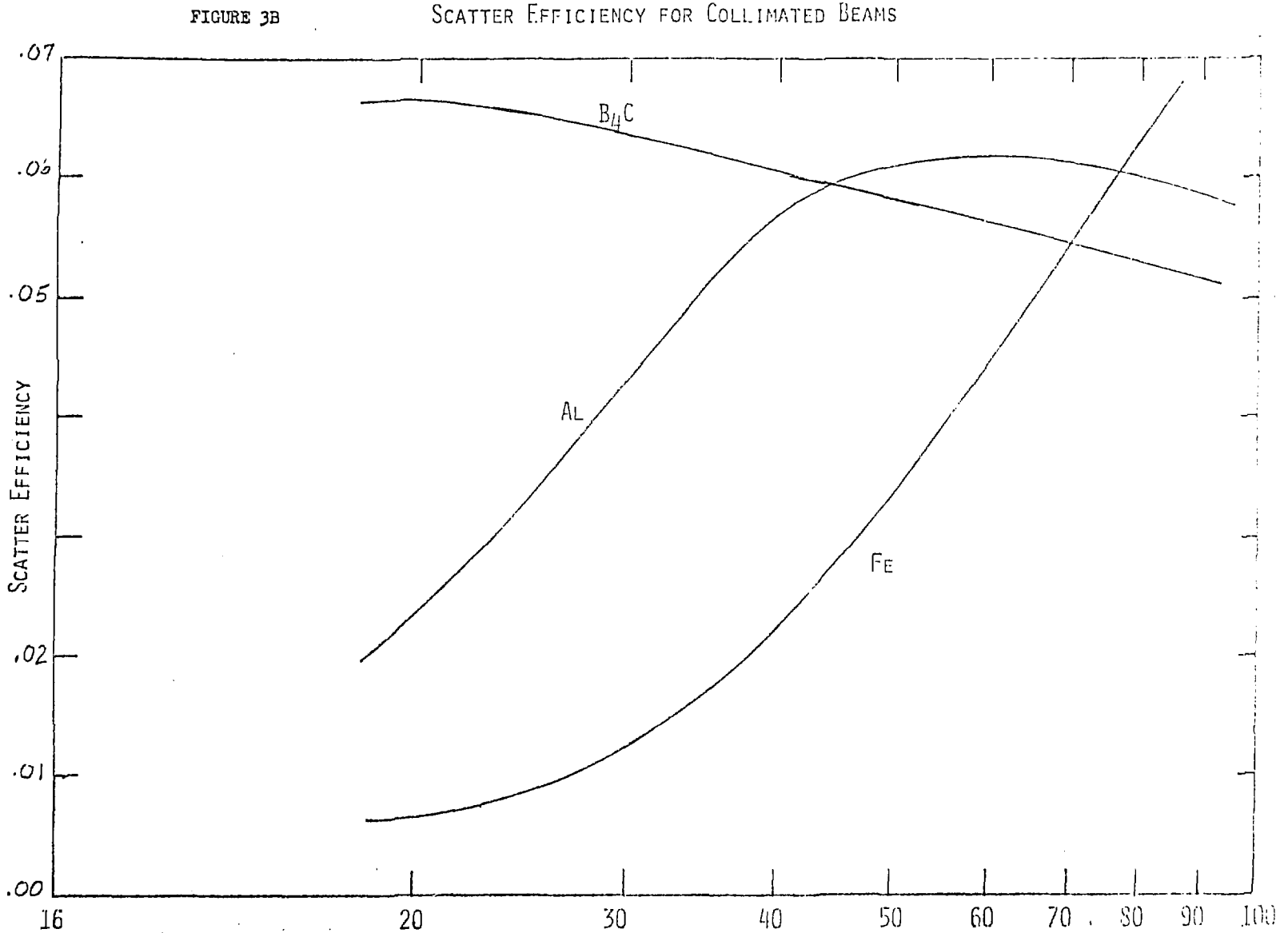
SCATTER EFFICIENCY FOR COLLIMATED BEAMS
SCATTER EFFICIENCY
.07
.06
.05
.02
.01
.00
16
20
30
40
50
60
70
80
90
100
B_4C
AL
FE

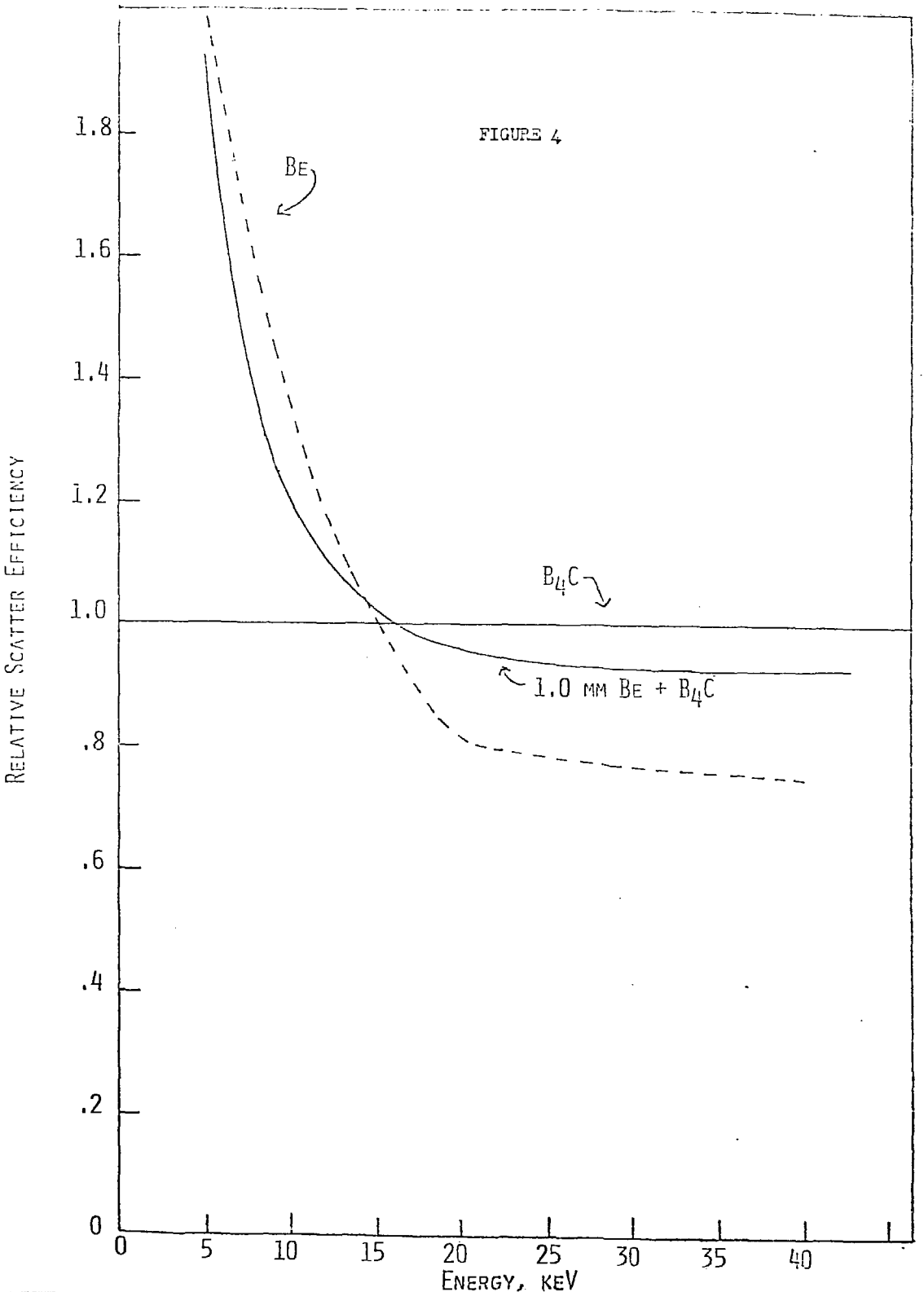
FIGURE 4
Be
B4C
1.0 mm Be + B4C
Relative Scatter Efficiency
Energy, keV
0
.2
.4
.6
.8
1.0
1.2
1.4
1.6
1.8
0
5
10
15
20
25
30
35
40

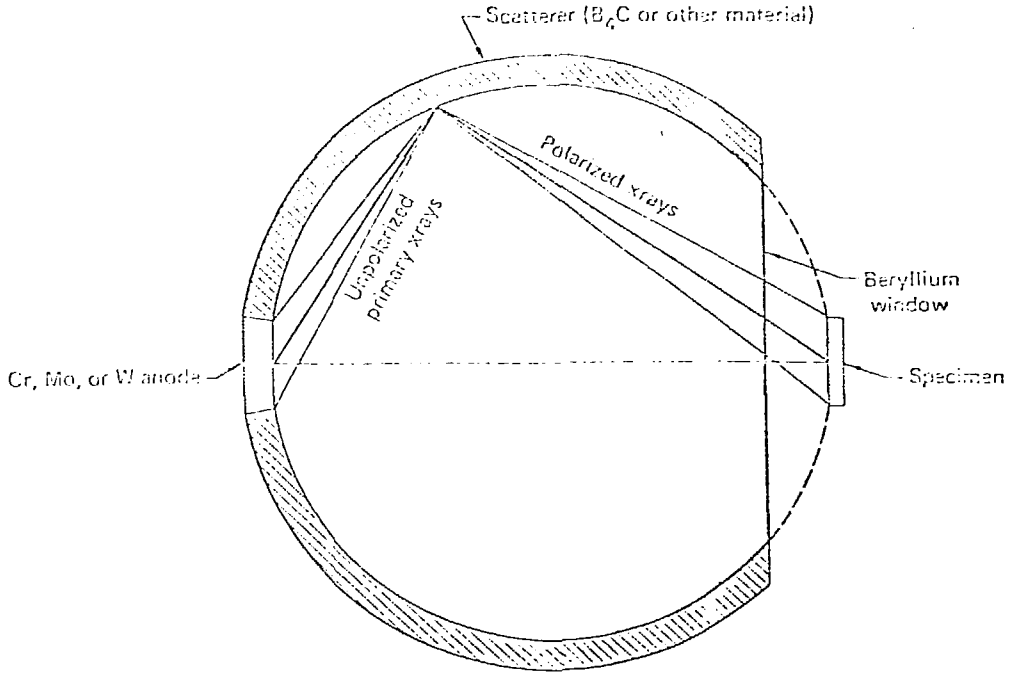
Scatterer (B_6C or other material)
Polarized xrays
Unpolarized primary xrays
Beryllium window
Cr, Mo, or W anode
Specimen

FIGURE 5.